AGU PUBLICATIONS

Geophysical Research Letters

RESEARCH LETTER
10.1002/2014GL059436

Key Points:
- Surface ocean biogeochemistry mediates physics of marine aerosol production
- Diel cycles in biologically productive surface seawater mediate production
- Observations show chemical processes affecting mass and number production fluxes

Supporting Information:
- Readme
- Text S1
- Figure S1
- Figure S2

Correspondence to:
M. S. Long,
mlong@seas.harvard.edu

Citation:
Long, M. S., W. C. Keene, D. J. Kieber, A. A. Frossard, L. M. Russell, J. R. Maben, J. D. Kinsey, P. K. Quinn, and T. S. Bates (2014), Light-enhanced primary marine aerosol production from biologically productive seawater, *Geophys. Res. Lett.*, *41*, 2661–2670, doi:10.1002/2014GL059436.

Received 28 JAN 2014
Accepted 20 MAR 2014
Accepted article online 27 MAR 2014
Published online 14 APR 2014

Light-enhanced primary marine aerosol production from biologically productive seawater

M. S. Long[1,2], W. C. Keene[2], D. J. Kieber[3], A. A. Frossard[4], L. M. Russell[4], J. R. Maben[2], J. D. Kinsey[3], P. K. Quinn[5], and T. S. Bates[6]

[1]School of Engineering and Applied Sciences, Harvard University, Cambridge, Massachusetts, USA, [2]Department of Environmental Sciences, University of Virginia, Charlottesville, Virginia, USA, [3]Department of Chemistry, College of Environmental Science and Forestry, State University of New York, Syracuse, New York, USA, [4]Scripps Institution of Oceanography, University of California, San Diego, California, USA, [5]Pacific Marine Environmental Laboratory, NOAA, Seattle, Washington, USA, [6]Joint Institute for the Study of the Atmosphere and Ocean, University of Washington, Seattle, Washington, USA

Abstract Physical and biogeochemical processes in seawater controlling primary marine aerosol (PMA) production and composition are poorly understood and associated with large uncertainties in estimated fluxes into the atmosphere. PMA production was investigated in the biologically productive NE Pacific Ocean and in biologically productive and oligotrophic regions of the NW Atlantic Ocean. Physicochemical properties of model PMA, produced by aeration of fresh seawater under controlled conditions, were quantified. Diel variability in model PMA mass and number fluxes was observed in biologically productive waters, increasing following sunrise and decreasing to predawn levels overnight. Such variability was not seen in oligotrophic waters. During daytime, surfactant scavenging by aeration in the aerosol generator without replenishing the seawater in the reservoir reduced the model PMA production in productive waters to nighttime levels but had no influence on production from oligotrophic waters. Results suggest bubble plume interactions with sunlight-mediated biogenic surfactants in productive seawater significantly enhanced model PMA production.

1. Introduction

Breaking waves on the ocean surface produce bubbles that burst at the air-sea interface and inject primary marine aerosol (PMA) into the atmosphere, ranging in size from 0.01 to 20 μm dry diameter [*Lewis and Schwartz*, 2004]. This process is the dominant source for aerosol mass and a major source for aerosol number in Earth's atmosphere with significant impacts on atmospheric chemistry and physics [*Lewis and Schwartz*, 2004; *Zhou et al.*, 2008].

Empirical relationships have been developed to predict size-resolved production fluxes of PMA as functions of near-surface wind speed, whitecap coverage [*Monahan and O'Muircheartaigh*, 1986; *Andreas*, 1998; *Vignati et al.*, 2001; *Gong*, 2003; *Mårtensson*, 2003; *Clarke et al.*, 2006; *Tyree et al.*, 2007], or wave-energy dissipation [*Long et al.*, 2011; *Norris et al.*, 2012]. PMA production is also influenced by surface-active organic matter in seawater that rapidly adsorbs onto surfaces of freshly produced bubbles, forming organic films that affect particle formation and associated chemical composition [*Adamson and Gast*, 1990; *Lewis and Schwartz*, 2004; *Modini et al.*, 2013]. Although research spanning several decades has studied various aspects of PMA production, we still do not understand how surface-ocean biogeochemistry and seawater organic matter (OM) affect PMA production and composition [*Hoffman and Duce*, 1976; *O'Dowd et al.*, 2004, 2008; *Gaston et al.*, 2011; *Long et al.*, 2011; *Gantt and Meskhidze*, 2013]. In this paper, we identify an important link between sunlight and surface-active OM that affected the physical production of PMA mass and number generated artificially from biologically productive seawater under controlled conditions.

2. Methods

PMA production was investigated during a cruise on the R/V *Atlantis*, as part of the 2010 California Nexus (CalNex) experiment, in the biologically productive eastern North Pacific Ocean off California from 15 May

to 6 June 2010 [*Bates et al.*, 2012] and during the Western Atlantic Climate Study (WACS) cruise on the R/V *Ronald H. Brown* in productive and oligotrophic regions of the northwestern Atlantic Ocean from 19 to 27 August 2012 [*Quinn et al.*, 2014] (Figure S1 in the supporting information). Model PMA (mPMA) were produced in a high-capacity generator fabricated from Pyrex and Teflon similar to that described in detail by *Keene et al.* [2007]. The generator used to produce mPMA is a closed system that excludes ambient air and solar radiation thereby minimizing chemical evolution other than dehydration of freshly produced aerosol. The generator was 20 cm in diameter and consisted of a seawater reservoir 122 cm deep underlying a 97 cm high atmosphere chamber. With the exception of several manipulation experiments (described below), fresh seawater from the ships' clean seawater lines (intake located approximately 5 m below the sea surface) flowed at 4 L min^{-1} into the base of the seawater reservoir and drained evenly over the top annular rim, continuously replacing the seawater surface and minimizing formation of standing bubble rafts. Ultrapure air hydrated to a relative humidity (RH) of 80 ± 2% flowed through the atmosphere above the seawater reservoir at rates of 48 to 70 L min^{-1} (rates varied based on the combined feed required by different sampling devices). Bubble plumes were generated by pumping ultrapure air through sintered glass frits positioned at an average depth of 84 cm below the air-seawater interface, which is within the range of ambient bubble-cloud depths generated by breaking waves on the open-ocean surface [*Thorpe*, 1982; *Thorpe et al.*, 1982; *Thorpe and Hall*, 1983]. mPMA were produced when the bubbles rose to and burst at the air-seawater interface. Aerosols were sampled for physical and chemical characterization through isokinetic ports at the top of the generator.

The original device described by *Keene et al.* [2007] was modified for shipboard deployment: (i) Overflow ports for seawater at the air-seawater interface were replaced with an annular space that allowed seawater exhaust to flow continuously across the entire circumference of the top edge of the Pyrex body at the top of the seawater reservoir. (ii) Teflon brackets were added to protect the glass frits from damage resulting from the ships' motion. (iii) The generator was supported within a rigid aluminum frame mounted on engineered shock absorbers and deployed in 20 foot shipping container configured as a laboratory van. (iv) To permit examining the effect of bubble size on particle production, options were added to produce bubbles with two independently regulated banks of fine-porosity frits (total of 11, 90 mm diameter, 10 to 20 μm pore size) and/or through one coarse-porosity frit (45 mm diameter, 145 to 174 μm pore size).

Seawater temperature, salinity, and chlorophyll *a* (Chl *a*) were measured continuously using employing flow-through systems. Chl *a* was calibrated based on intermittent analysis of discrete samples [*Bates et al.*, 2012]. Solar radiation was measured continuously with an Epply model 8-48 Black and White Pyranometer and an Epply model PSP Precision Spectral Pyranometer. Seawater-dissolved organic carbon (DOC) was measured with a Shimadzu Model TOC-V CSH high-temperature combustion carbon analyzer [*Keene et al.*, 2007]. Bubble sizes within 2 to 4 cm of the air-water interface within the generator were quantified using computer-enhanced camera images and *ImageJ* software (http://rsb.info.nih.gov/ij/index.html).

Dynamic bubble surface tension in seawater was measured during the WACS cruise with a Sensadyne Model QC-6000 maximum bubble pressure method surface tensiometer calibrated with 18 MΩ ultrapure water (hereafter referred to as deionized water (DIW)) and reagent grade isopropyl alcohol (BDH, CAS 67-63-0). Bubbles were generated using dual quartz capillary tubes with radii of 0.25 mm and 2.0 mm, and dry air (dewpoint −26.7°C) set to 2.38 atm. Capillaries were submerged approximately 4 cm into 50 mL aliquots of untreated, room-temperature seawater samples held in an acid-cleaned fluorinated polyethylene vessel. The sample temperature was monitored continually. Standards were analyzed after each sample. If standards varied by more than 0.1 mN m^{-1}, the QC-6000 was recalibrated and the sample reanalyzed. Seawater samples were taken from the ship's continuous-flow seawater system and from the port bow ahead of any ship effluent using an acid-washed FPE bottle. Samples not analyzed within 2 h of collection were stored at 5°C for analysis within 6 h of collection or frozen at −20°C and analyzed within 24 h. Dynamic surface tension was recorded to within 0.1 mN m^{-1} at various bubble surface ages.

Generated mPMA were sampled for chemical characterization over nominal 22 h periods with a nonrotating Multi-orifice Uniform Deposit Impactor (MOUDI) operating at 30 L min^{-1} [*Marple et al.*, 1991]. The 50% aerodynamic diameter cut sizes were 0.18, 0.32, 0.56, 1.00, 1.8, 3.2, 5.6, 10.0, and 18 μm. During both cruises, the MOUDI was configured with precombusted 47 mm diameter aluminum substrates and 37 mm diameter quartz backup filters for analysis of organic carbon. Exposed samples were transferred to

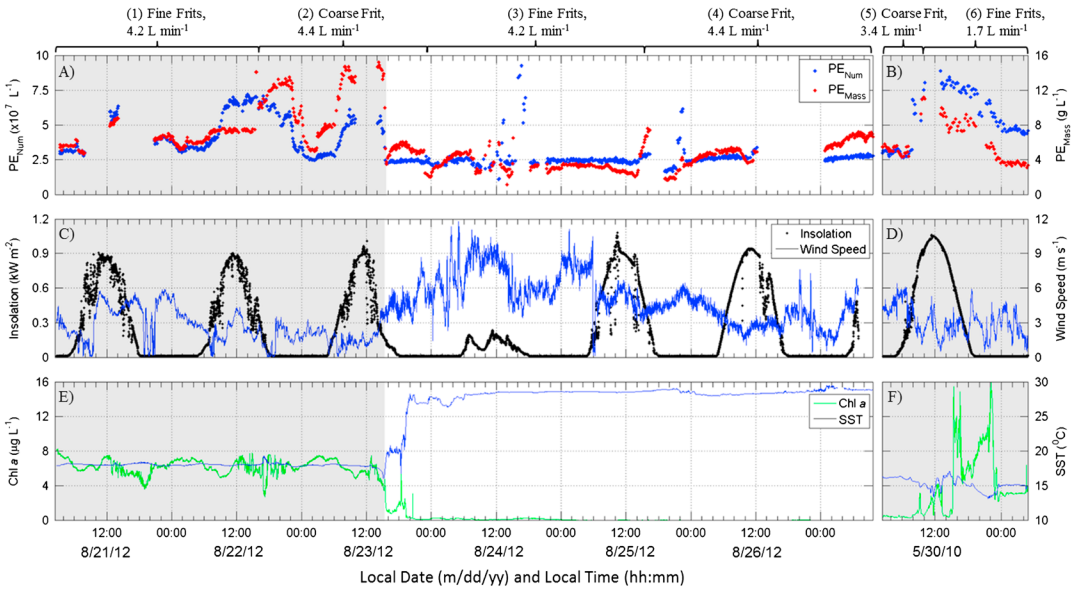

Figure 1. Time series of PE_{Num} and PE_{Mass} during (a) WACS and (b) CalNex, corresponding (c) insolation and (d) wind speed during WACS and CalNex, respectively, and (e) Chl *a* and (f) SST. Numbered brackets at top of Figures 1a and 1b bound measurements under identical operating conditions as indicated. Shaded regions depict productive waters including WACS-S1, first leg of transit to WACS-S2, and CalNex. Breaks in the time series correspond to changes in operating conditions to evaluate other characteristics of the system, power outages, and instrument malfunctions.

precombusted 10 mL Pyrex centrifuge tubes, extracted immediately in 5 mL of DIW, stored frozen, and analyzed for organic carbon (OC) at the State University of New York (SUNY) using a Shimadzu high-temperature combustion carbon analyzer. Aerosols were also sampled in bulk at 30 L min^{-1} over nominal 12 h periods on precombusted 47 mm diameter quartz fiber filters and similarly handled and analyzed for OC at SUNY and for major ions by ion chromatography at the University of Virginia. Periodically, the feed seawater for the aerosol generator was filtered through a precleaned, 0.2 μm Whatman POLYCAP 75 AS filter capsule and analyzed for DOC.

mPMA number size distributions in the generator head space were measured continuously from 0.01 to 15 μm dry diameter with a TSI model 3321 Aerodynamic Particle Sizer and a Scanning Mobility Particle Sizer (Bretchel Manufacturing, Inc.) using a 5 min integration time. The production efficiency of mPMA number per unit volume of air detrained (PE_{Num}, in units of L^{-1}) was calculated directly from the measured number size distribution and the corresponding air detrainment rate (detrainment is defined as the rate at which bubbled exited the generator's seawater reservoir across the air-water interface). The corresponding production efficiency of mPMA mass (PE_{Mass} in units of g L^{-1}) was calculated based on the measured volume size distribution, a density of 2.14 g cm^{-3} for particles ≥1 μm diameter (that were dominated by inorganic sea salt), a density of 1.84 g cm^{-3} for particles ≤ 1 μm diameter, and the corresponding air detrainment sampling rate. The lower density for particles ≤1 μm diameter reflects contributions by OM with an assumed density of 1.1 g cm^{-3} [*Schkolnik et al.*, 2007].

3. Results

A distinguishing feature of WACS was the persistence of low winds and calm seas (Figure 1c). Relative to more energetic sea states, influences on near-surface surfactant OM by wind-driven vertical mixing and wave-breaking aeration of near-surface seawater were minimal, thereby providing better resolution for evaluating relationships between surface mixed layer seawater characteristics and PMA production. Over one complete 24 h period (22 August 2012) at WACS Station 1 (denoted hereafter as WACS-S1) in association with high algal biomass (based on Chl *a*, Figure 1e), PE_{Mass} and PE_{Num} (collectively referred to as PE) in the generator increased rapidly at sunrise and decreased overnight (Figure 1 and Table 1). Discontinuous measurements on 21 and 23 August suggest similar diel cycles in the aerosol generator at this station. During the afternoon of

Table 1. Diel Variability in Mean PE_{Num} and PE_{Mass} (± Standard Deviations) During WACS-S1, WACS-S2, and CalNex and Corresponding Meteorological Conditions and Seawater Characteristics

	WACS-S1[a]	WACS-S1[b]	WACS-S2[c]	CalNex[d]
Wind speed ($m\,s^{-1}$)	3.2 ± 1.5	1.7 ± 0.76	5.1 ± 1.1	3.4 ± 1.9
Maximum insolation ($W\,m^{-2}$)	904	964	1005	1159
SST (°C)	18.0 ± 0.1	18.0 ± 0.2	24.6 ± 3.4	15.3 ± 0.84
Chl *a* ($\mu g\,L^{-1}$)	6.2 ± 0.82	6.1 ± 0.26	0.10 ± 0.32[e]	3.2 ± 3.1
Seawater DOC (μM)	86.7 ± 1.0 (*N* = 2)	89.7 ± 3.3 (*N* = 2)	73.4 ± 3.6 (*N* = 4)	62.2 ± 3.9 (*N* = 5)
PE_{Num}, daytime[f] ($\times 10^7\,L^{-1}$)	6.0 ± 0.99	5.9 ± 0.57	2.3 ± 3.4	7.5 ± 0.62
PE_{Num}, nighttime[bg] ($\times 10^7\,L^{-1}$)	3.3 ± 0.31	2.9 ± 0.37	2.7 ± 0.5	3.1 ± 0.3
PE_{Mass}, daytime[f] ($g\,L^{-1}$)	7.1 ± 0.69	12.8 ± 1.2	2.2 ± 0.9	8.6 ± 1.1
PE_{Mass}, nighttime[g] ($g\,L^{-1}$)	5.4 ± 0.38	6.7 ± 1.1	3.5 ± 2.7	5.0 ± 0.4
Peak PE_{Num}, D_{dry}[h] (μm)	0.069 ± 0.01 (*N* = 286)	0.089 ± 0.01 (*N* = 210)	0.073 ± 0.01 (*N* = 854)	0.080 ± 0.020 (*N* = 122)
Peak PE_{Mass}, D_{dry}[h] (μm)	1.14 ± 0.05 (*N* = 286)	1.14 ± 0.05 (*N* = 210)	1.17 ± 0.19 (*N* = 854)	1.03 ± 0.03 (*N* = 122)

[a]Bracketed interval 1 depicted in Figure 1.
[b]Shaded portion of bracketed interval 2 depicted in Figure 1.
[c]Unshaded portion of bracketed intervals 2–4 depicted in Figure 1; excludes periods of sporadic behavior between 10:00 and 17:00 on 24 August 2012 and between 1400 and 2200 on 25 August 2012.
[d]Bracketed intervals 5 and 6 depicted in Figure 1.
[e]Chl *a* in this interval were lognormally distributed with a distribution of $10^{-1.1\pm0.6}\,\mu g\,L^{-1}$.
[f]Mean (± standard deviation) for measurements depicted in Figure 1 during the period starting 4 h following sunrise through 2 h following sunset.
[g]Mean (± standard deviation) for measurements depicted in Figure 1 during 6 h period preceding sunrise.
[h]Dry diameter.

23 August, abrupt, nearly stepwise reductions in PE_{Mass} and PE_{Num} occurred during the ship's transit from biologically productive waters at WACS-S1 to oligotrophic waters in the Sargasso Sea at WACS Station 2 (denoted hereafter as WACS-S2). This transit coincided with sharp changes in seawater Chl *a* and sea surface temperature (SST) (Figure 1e). Thereafter, and with the exception of two relatively brief periods of sporadic variability, relatively low and nearly constant PE persisted for more than 3 days at the WACS-S2 station (Figure 1a and Table 1). Corresponding frequency distributions for PE_{Num} revealed distinct modes during daytime and nighttime at WACS-S1 (Figures 2a and 2b) that indicated the influence of an active process modulating PE_{Num} over diel cycles. No such diel variability was evident at WACS-S2 in the aerosol generator (Figure 2c).

During CalNex, more variable Chl *a* and SST were encountered relative to WACS, reflecting the seawater heterogeneity from upwelling along the California coast; wind speeds and sea states also varied widely [*Bates et al.*, 2012]. Under higher wind conditions (greater than ~4 $m\,s^{-1}$), there is evidence suggesting diel variations in PE (Figure S2) similar to those observed during quiescent conditions at WACS-S1, although changes to instrumentation and generator settings during this period prohibited interpreting these data unequivocally. However, over one 24 h period, on 30 May 2010 during which sea state was generally calm, PE exhibited a diel trend similar to that observed in productive waters at WACS-S1 (Figures 1b and 2d and Table 1).

We note that discontinuities in the PE time series (primarily PE_{Mass}) are clearly visible in Figures 1 and S1 and that they correspond to changes in frit sizes as indicated by the brackets along the top of the figures. These discontinuities are primarily due to changing bubble sizes and corresponding bubble surface area and lifetimes, as well as air detrainment rates.

Dynamic bubble surface tension [*Adamson and Gast*, 1990], at surface ages ranging from 0.1 to 4 s, was measured throughout the WACS campaign. Due to method limitations at sea, dynamic surface tension could not be quantified within the range of bubble lifetimes in the generator (10 to 20 s, see the supporting information for discussion of bubble sizes and lifetimes). Thus, dynamic surface tension cannot be compared directly to corresponding PEs. Nonetheless, under all conditions in biologically productive and oligotrophic waters, dynamic surface tension ranged from 0.4 to 1.2 $mN\,m^{-1}$ below that of seawater at ambient temperature and equivalent salinity but with no surfactants, indicating that surfactants were always present on bubble surfaces, independent of seawater trophic state.

To evaluate the nature of diel variability in greater detail, influences of surfactant depletion via bubble scavenging on PE during daytime were quantified by turning off the seawater flow through the generator for

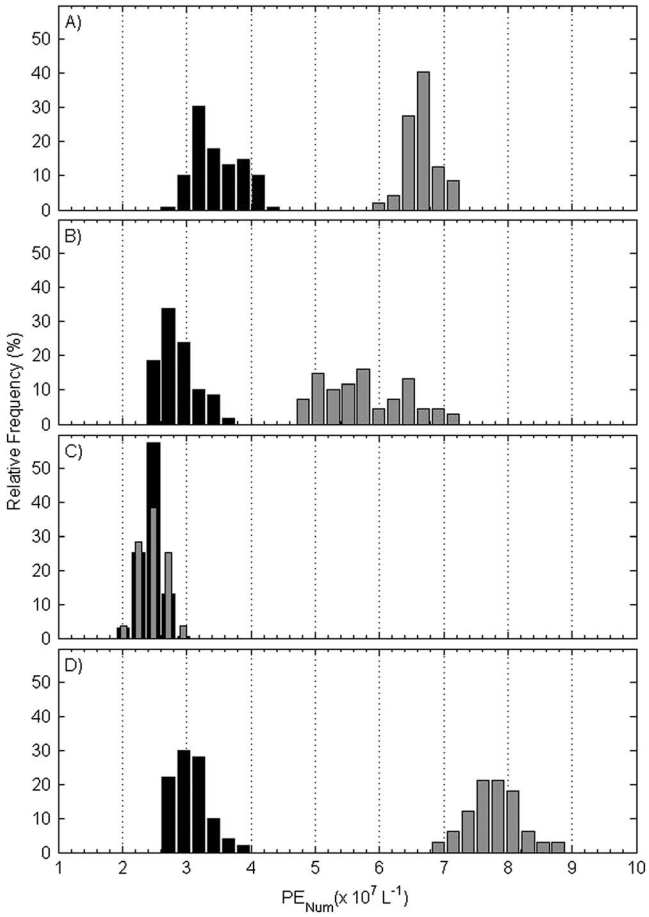

Figure 2. Frequency distributions of PE_{Num} for (a) WACS-S1, interval1I in Figure 1, (b) WACS-S1, shaded portion of interval 2 in Figure 1, (c) WACS-S2, and (d) CalNex corresponding to the time periods from which PE_{Num} values in Table 1 were calculated. Black and gray bars represent PE_{Num} during the nighttime and daytime periods, respectively, as specified in Table 1.

approximately 30 min each at WACS-S1 and WACS-S2 and approximately 60 min each over two discrete intervals during CalNex; thereafter, continuous seawater flow was restored. These nonflowing conditions are comparable to those in previous studies that employed aerosol generators with fixed volumes of seawater that were not replenished, during which adsorption of seawater surfactants onto bubble surfaces and transport to the surface depleted surfactant concentrations in bulk solution [*Skop et al.*, 1994; *Stefan and Szeri*, 1999].

Under nonflowing conditions in productive waters at WACS-S1 and during CalNex, PE_{Num} decreased sharply and then recovered toward lower steady state values (Figures 3a and 3c and Table 2). When flowing seawater was restored in the generator, PE_{Num} quickly returned to higher initial levels. The corresponding PE_{Mass} decreased sharply to near-zero and gradually increased to lower values in a pattern similar to PE_{Num}, returning to initial conditions when seawater flow was restored (Figures 3a and 3c and Table 2). Initial rapid drops and subsequent increase in PEs immediately after the seawater flow was turned off were likely due to accumulation of surfactant material at the seawater-air interface resulting in thickened bubble rafts that temporarily slowed aerosol production. Continued emission of surface-active OM across the interface depleted the initial excess, eroded the raft, and allowed the system to equilibrate toward a new steady state. This did not occur when seawater flow was on because the balance of surfactant delivered to the surface but not injected across the interface drained to waste with the seawater exhaust, with no buildup of surfactants at the interface. These results (Figures 3a and 3c and Table 2) suggest that surfactants sustaining higher PE under flowing conditions were depleted via bubble scavenging when the seawater was not flowing, revealing the influence of another, distinctly different surfactant reservoir that sustained lower PEs.

In marked contrast to WACS-S1 at Georges Bank, PE_{Num} increased to slightly higher, marginally significant ($p = 0.03$) levels at the oligotrophic seawater station WACS-S2 when the seawater flow was turned off, while PE_{Mass} exhibited no significant change ($p = 0.6$; Figure 3c and Table 2). These results suggest that, unlike in productive waters, depletion of surfactants via bubble scavenging in oligotrophic waters did not alter PEs. In addition, under nonflowing conditions, PE_{Num} for WACS-S1 and WACS-S2 was statistically indistinguishable ($p = 0.73$), and size-resolved PE_{Num} values for productive waters at WACS-S1 and during CalNex rapidly converged (5 to 10 min) toward those at WACS-S2 (Figure 4 and Table 2). During nonflowing conditions at all three stations (Table 2), average PE_{Num} values also fell within the range of corresponding average PE during late night with flowing seawater (Figure 1 and Table 1). Nonflowing PE_{Mass} differed to a greater degree among experiments (Table 2), and all PE_{Mass}

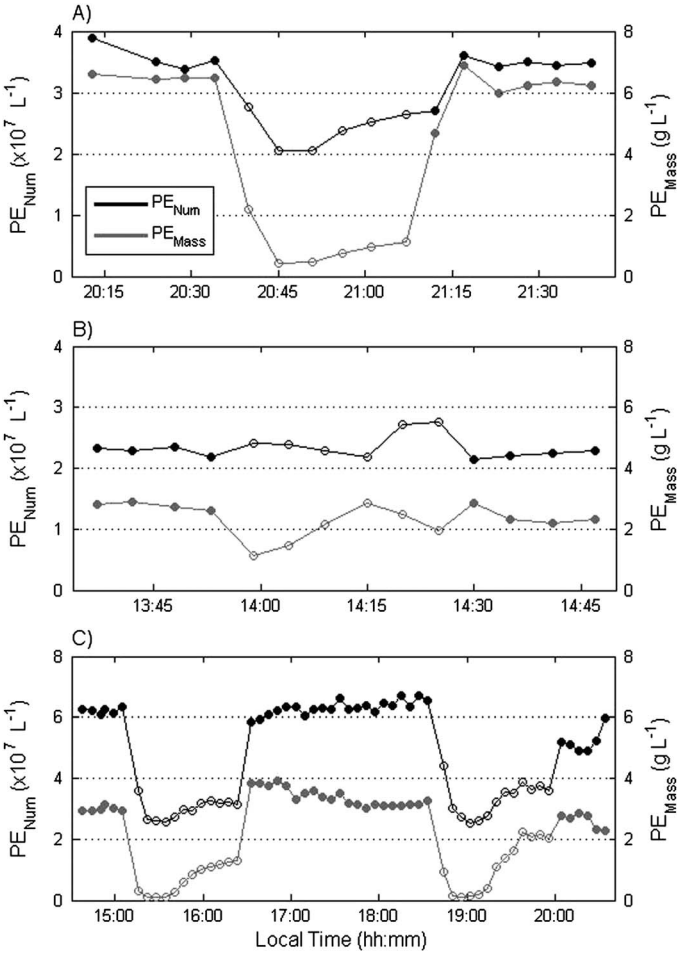

Figure 3. Time series of PE_{Num} and PE_{Mass} during the seawater on-off experiments: (a) WACS-S1 on 20 August 2012, (b) WACS-S2 on 24 August 2012, and (c) CalNex on 6 June 2010. Solid symbols depict PE with seawater flow on and open symbols with seawater flow off. Note that scales on *Y* axes differ.

values were lower than those measured during late night with flowing seawater (Table 1). This unexpected finding indicates that OM, which accounts for only a minor component of total marine aerosol mass [*Keene et al.*, 2007; *Facchini et al.*, 2008], played a direct role in mPMA production over diel cycles in productive waters.

4. Discussion

Results from time series measurements (Figures 1 and 2) and experiments with the seawater intake flow turned on and off (Figures 3 and 4) suggest that large diel variability in PE_{Num} and PE_{Mass} measured in productive marine waters was driven by diel changes in surfactant composition. This interpretation is consistent with changes in bubble sizes measured during the on-off experiment at WACS-S1. Volumes of individual bubbles measured within 2 to 4 cm below the air-water interface were significantly greater ($p \ll 0.01$) in nonflowing seawater relative to those during flowing conditions (Table 2) even though the corresponding ionic composition and temperature of seawater did not vary. This behavior is consistent with the Young-Laplace relationship that relates the bubble radius to surface tension, as they are affected by the concentration and composition of surfactants in the water [*Adamson and Gast*, 1990; *Burns and Zhang*, 2001]. Bubble sizes were not measured during the on-off experiments for CalNex or WACS-S2. We thus infer that changes in bubble size under flowing versus nonflowing conditions at WACS-S1 were driven primarily by changes in the surfactant OM composition of seawater and associated dynamic bubble surface tension. We return to this issue below.

Measured diel trends in PE for biologically productive regions provide direct evidence for a sunlight-mediated process that results in the formation of surfactant OM in the surface ocean that modulates the

Table 2. Mean PE_{Num}, PE_{Mass}, and Bubble Volume (± Standard Deviation) Under Flowing and Nonflowing Seawater Conditions Within the Generator[a]

	Flowing Seawater			Nonflowing Seawater		
	PE_{Num} ($\times 10^7$ L^{-1})	PE_{Mass} (g L^{-1})	Bubble Volume (mm^3)	PE_{Num}[b] ($\times 10^7$ L^{-1})	PE_{Mass}[b] (g L^{-1})	Bubble Volume (mm^3)
WACS-S1	3.4 ± 0.3	6.2 ± 0.6	0.016 ± 0.005 (N = 91)	2.5 ± 0.1	0.95 ± 0.19	0.036 ± 0.012 (N = 48)
WACS-S2	2.3 ± 0.1	2.6 ± 0.3	N/A	2.5 ± 0.2	2.0 ± 0.6	N/A
CalNex	6.1 ± 0.5	3.2 ± 0.4	N/A	3.5 ± 0.1	1.6 ± 0.7	N/A

[a]For all experiments, bubbles were generated by pumping ultrapure air through fine frits at 4.2 L min^{-1}; when on, seawater flow was at 4.0 L min^{-1}.
[b]Statistics based on final three measurements with nonflowing seawater.

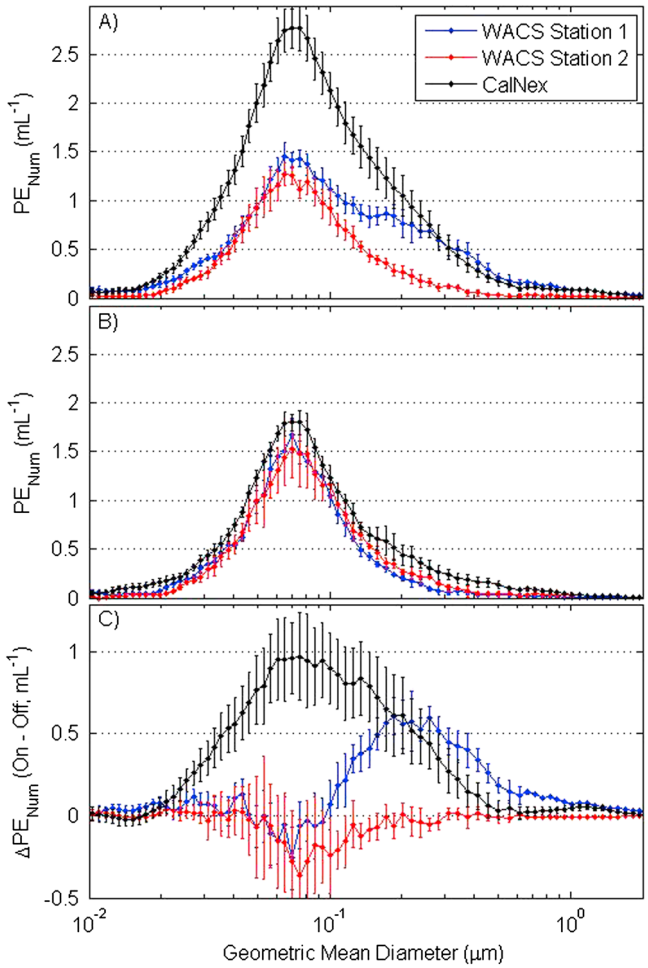

Figure 4. Mean size-resolved PE_{Num} during seawater on-off experiments with (a) flowing seawater, (b) nonflowing seawater, and (c) the corresponding difference ($\Delta PE_{Num} = PE_{Num}$ in Figure 4a minus PE_{Num} in Figure 4b). PE_{Num} in Figure 4b corresponds to the final three observations with nonflowing seawater (open circles, Figure 3).

physics of PMA production. Unfortunately, insufficient data were available to quantify diel cycling in the PMA organic fraction. The ratio of organic matter to inorganic sea salt in mPMA produced by our generator and by a marine aerosol generator deployed at the sea surface (SeaSweep) was unchanged between WACS-S1 and WACS-S2 [*Quinn et al.*, 2014], implying that the mechanism linking marine surfactant OM to PMA production involves surfactant interactions at bubble surfaces. The absence of diel PE variability in oligotrophic seawater indicates that this sunlight-driven process is not universally important in the surface ocean but rather is associated with productive marine waters. Even though OM enrichments relative to inorganic sea salt do not differ over a wide range of surface-ocean algal biomass [*Quinn et al.*, 2014], our results suggest that sunlight should enhance PMA production in biologically productive waters, increasing sea-air OM emission fluxes.

This process is particularly interesting because of the combined influence on both the number and mass production fluxes of mPMA. In the atmosphere, PMA number fluxes are dominated by submicrometer diameter particles composed primarily of OM, whereas mass fluxes are dominated by supermicrometer diameter particles composed primarily of inorganic sea salt [*Keene et al.*, 2007; *Yoon et al.*, 2007; *Facchini et al.*, 2008; *Quinn et al.*, 2014]. Given the relatively large contribution of OM to submicrometer PMA that dominates number fluxes, a sensitivity of PE_{Num} to seawater OM may be expected. However, large influences of seawater OM on PE_{Mass} in productive waters were surprising given the minor contribution of OM to PMA mass (i.e., a few percent [*Keene et al.*, 2007; *Facchini et al.*, 2008]). Concentrations of DOC in feed seawater (Table 1) measured in parallel with mPMA production fluxes and composition at all stations indicated that emission

fluxes of particulate OM across the air-water interface via bursting bubbles corresponded to less than 0.01% of the DOC flux through the generator when seawater flow was on. Assuming similar production fluxes of particulate OM when the seawater was not flowing, less than 0.03% of the DOC was emitted to the overlying atmosphere during 30 to 60 min periods with no seawater flow. It is evident that although only trace amounts of OM in seawater were injected across the air-water interface under these conditions, the surfactants involved in this process had a disproportionately large impact on the physics of mPMA production. This result is inconsistent with previous work that suggests OM plays a strictly passive role in PMA production [*Gantt et al.*, 2009; *Long et al.*, 2011; *Ault et al.*, 2013].

Measured surface tensions indicate that surface-active organics coated bubble surfaces under all experimental conditions during WACS, which (together with the above results) suggests that surfactants influence PE in both productive and oligotrophic waters. A reservoir of sunlight-generated surfactants drives enhanced PE during the daytime and early evening in productive waters, superimposed upon a "background" of diurnally stable surfactants that sustain lower PE during late night. Comparison of PE_{Num} frequency and size distributions suggests that sunlight-mediated surfactants have distinct influences on PMA production that vary geographically (Figures 2, 4a, and 4c). Minor variability in PE in Figure 2 (black bars) likely reflects small differences in background surfactant concentrations or speciation coupled with variability in physical conditions (water temperature and salinity). While background PE_{Num} for each station differed significantly ($p > 0.1$), overlapping ranges (Table 1 and 2) combined with the similarity among the number size frequency distributions (Figure 4) suggest that the background surfactants may be similar. These results raise three important questions: (1) What is the nature of the sunlight-mediated surfactant source(s) in productive waters? (2) By what mechanism(s) do the surfactants control the observed variability in PE? (3) What is the composition and source of the background reservoir(s) of surfactants that appear to be decoupled from biological or photochemical processes on daily time scales?

Our results suggest that the sunlight-mediated surfactants in biologically productive waters originated from biological and/or photochemical processes. Although the production pathways are not known, it is clear that associated dynamics are not captured by simple biological proxies such as Chl *a*. Diel cycling of PE in our generator did not vary in response to changes in SST and Chl *a* during CalNex (Figures 1b and 1f) suggesting that changes in local water origin and associated algal biomass are not primary controlling factors in productive waters. The abrupt decrease in PE in transition from WACS-S1 to WACS-S2 occurred at relatively high concentrations of Chl *a* (mean of 1.5 $\mu g\, L^{-1}$ between 15:30 and 19:00 on 23 August; Figure 1e), which are at or greater than concentrations used by other investigators to justify Chl *a* as a good proxy of organic PMA enrichment relative to inorganic sea salt [*O'Dowd et al.*, 2004; *Facchini et al.*, 2008; *Long et al.*, 2011; *Rinaldi et al.*, 2013].

The mechanism by which organic surfactants modulate the physical production of PMA number and mass is uncertain, especially considering that bubble bursting at the sea surface often occurs within rafts of interacting bubbles whose "bursting" properties are different from individual bubbles [*Ghosh*, 2004]. Surface-active OM in seawater rapidly adsorbs onto freshly produced bubble surfaces forming organic films that mediate bubble size in the water column and bubble evolution and lifetime at the sea surface [*Adamson and Gast*, 1990; *Lewis and Schwartz*, 2004; *Modini et al.*, 2013]. The influence of surface-active OM on the physical process of bubble bursting at the sea surface is attributed in part to control of bubble size and the associated delivery of organic-coated bubble surface area to the air-sea interface. Thus, with flowing seawater at WACS-S1, the smaller bubble size (Table 2) and larger bubble surface area delivered to the air-water interface per unit air detrained may have contributed to the higher PEs relative to nonflowing conditions (Figure 3a). In addition, the potential energy available for a given bubble to produce particles is the buoyant force for the fraction of the bubble submerged beneath the surface counteracted by the surface tension of the film cap [*Duchemin et al.*, 2002; *Lewis and Schwartz*, 2004]. As the film cap drains and thins, its capacity to counteract buoyancy decreases, thereby diminishing the buoyant energy and the energy and mass of the bubble cap. Bubble stability characteristics and the associated energy available to produce new particles vary as a function of the chemical properties of organic surfactants that produce films [*Garrett*, 1967; *Modini et al.*, 2013]. Thus, for a given set of conditions, surfactants produced in productive waters during daytime may sustain higher PE than surfactants associated with the background OM at night in productive and oligotrophic waters.

Direct extrapolation of these results to the ambient air-sea interface is constrained by the limited range of conditions evaluated and because surfactants also influence wind-wave formation and breaking, and subsequent bubble plume generation and evolution [*Hara et al.*, 1997; *Deane and Stokes*, 1999; *Loewen*, 2002; *Liu and Duncan*, 2003; *Frew*, 2004; *Callaghan et al.*, 2008; *Salter et al.*, 2011], which cannot be characterized with the marine aerosol generator as currently configured. However, our results clearly indicate the presence of at least two distinct reservoirs of surface-active OM in the biologically productive waters: one of which is controlled by solar radiation in the surface ocean. The effect of solar radiation on the production of surfactant OM, possibly through a biological process that is coupled to or independent from photochemical OM transformations, diurnally modulates the production of mPMA mass and number from productive waters but not oligotrophic waters. This large and previously unrecognized source of variability potentially contributes to the wide range in reported PEs under otherwise similar conditions [*Lewis and Schwartz*, 2004]. Future work will help resolve the nature of this light-driven process and its impact on ambient PMA production in conjunction with known physical drivers.

Acknowledgments

We thank G. Henderson, I. Tyssebotn, D. Coffman, K. Schulz, D. Hamilton, J. Johnson, and M. Haserodt for their assistance in sample collection and analysis; V. Trainer for the loan and calibration of the fluorometer; and the captains and crews of the NOAA R/V *Ronald H. Brown* and the UNOLS R/V *Atlantis* for logistical support in the field. We also thank S. Loucaides, J. Willey, R. Kieber, and W. Miller for helpful discussions regarding marine chemistry. Primary financial support for this work was provided by the U.S. National Science Foundation through awards to the University of Virginia (OCE-0948420 and OCE-1129836), SUNY ESF (OCE-0948216 and OCE-1129896), Scripps Institute of Oceanography (OCE-1129580), and Harvard University (AGS-1252755). Additional support was provided by the NOAA Atmospheric Composition and Climate Program.

The Editor thanks two anonymous reviewers for their assistance in evaluating this paper.

References

Adamson, A. W., and A. P. Gast (1990), *Physical Chemistry of Surfaces*, Wiley, New York.

Andreas, E. L. (1998), A new sea spray generation function for wind speeds up to 32 m s^{-1}, *J. Phys. Ocean.*, *28*(11), 2175–2184.

Ault, A. P., et al. (2013), Size-dependent changes in sea spray aerosol composition and properties with different seawater conditions, *Environ. Sci. Technol.*, *47*(11), 5603–5612, doi:10.1021/es400416g.

Bates, T. S., et al. (2012), Measurements of ocean derived aerosol off the coast of California, *J. Geophys. Res.*, *117*, D00V15, doi:10.1029/2012JD017588.

Burns, S. E., and M. Zhang (2001), Effects of system parameters on the physical characteristics of bubbles produced through air sparging, *Environ. Sci. Technol.*, *35*(1), 204–208, doi:10.1021/es001157u.

Callaghan, A., G. de Leeuw, L. Cohen, and C. D. O'Dowd (2008), Relationship of oceanic whitecap coverage to wind speed and wind history, *Geophys. Res. Lett.*, *35*, L23609, doi:10.1029/2008GL036165.

Clarke, A. D., S. R. Owens, and J. Zhou (2006), An ultrafine sea-salt flux from breaking waves: Implications for cloud condensation nuclei in the remote marine atmosphere, *J. Geophys. Res.*, *111*, D06202, doi:10.1029/2005JD006565.

Deane, G. B., and M. D. Stokes (1999), Air entrainment processes and bubble size distributions in the surf zone, *J. Phys. Ocean.*, *29*(7), 1393–1403.

Duchemin, L., S. Popinet, C. Josserand, and S. Zaleski (2002), Jet formation in bubbles bursting at a free surface, *Phys. Fluids*, *14*, 3000.

Facchini, M. C., et al. (2008), Primary submicron marine aerosol dominated by insoluble organic colloids and aggregates, *Geophys. Res. Lett.*, *35*, L17814, doi:10.1029/2008GL034210.

Frew, N. M. (2004), Air-sea gas transfer: Its dependence on wind stress, small-scale roughness, and surface films, *J. Geophys. Res.*, *109*, C08S17, doi:10.1029/2003JC002131.

Gantt, B., and N. Meskhidze (2013), The physical and chemical characteristics of marine primary organic aerosol: A review, *Atmos. Chem. Phys.*, *13*(8), 3979–3996, doi:10.5194/acp-13-3979-2013.

Gantt, B., N. Meskhidze, and D. Kamykowski (2009), A new physically-based quantification of marine isoprene and primary organic aerosol emissions, *Atmos. Chem. Phys.*, *9*(14), 4915–4927, doi:10.5194/acp-9-4915-2009.

Garrett, W. D. (1967), Stabilization of air bubbles at the air-sea interface by surface-active material, *Deep Sea Res. Ocean. Abstr.*, *14*(6), 661–672, doi:10.1016/S0011-7471(67)80004-4.

Gaston, C. J., H. Furutani, S. A. Guazzotti, K. R. Coffee, T. S. Bates, P. K. Quinn, L. I. Aluwihare, B. G. Mitchell, and K. A. Prather (2011), Unique ocean-derived particles serve as a proxy for changes in ocean chemistry, *J. Geophys. Res.*, *116*, D18310, doi:10.1029/2010JD015289.

Ghosh, P. (2004), A comparative study of the film-drainage models for coalescence of drops and bubbles at flat interface, *Chem. Eng. Technol.*, *27*(11), 1200–1205, doi:10.1002/ceat.200402143.

Gong, S. L. (2003), Canadian Aerosol Module: A size-segregated simulation of atmospheric aerosol processes for climate and air quality models 1. Module development, *J. Geophys. Res.*, *108*(D1), 4007, doi:10.1029/2001JD002002.

Hara, T., E. J. Bock, and M. Donelan (1997), Frequency-wavenumber spectrum of wind-generated gravity-capillary waves, *J. Geophys. Res.*, *102*(C1), 1061–1072, doi:10.1029/96JC03229.

Hoffman, E. J., and R. A. Duce (1976), Factors influencing the organic carbon content of marine aerosols: A laboratory study, *J. Geophys. Res.*, *81*(21), 3667–3670, doi:10.1029/JC081i021p03667.

Keene, W. C., et al. (2007), Chemical and physical characteristics of nascent aerosols produced by bursting bubbles at a model air-sea interface, *J. Geophys. Res.*, *112*, D21202, doi:10.1029/2007JD008464.

Lewis, E. R., and S. E. Schwartz (2004), *Sea Salt Aerosol Production: Mechanisms, Methods, Measurements, and Models - A Critical Review*, *Geophys. Monogr. Ser.*, vol. 152, AGU, Washington, D. C.

Liu, X., and J. H. Duncan (2003), The effects of surfactants on spilling breaking waves, *Nature*, *421*(6922), 520–523, doi:10.1038/nature01357.

Loewen, M. (2002), Physical oceanography: Inside whitecaps, *Nature*, *418*(6900), 830–830.

Long, M. S., W. C. Keene, D. J. Kieber, D. J. Erickson, and H. Maring (2011), A sea-state based source function for size- and composition-resolved marine aerosol production, *Atmos. Chem. Phys.*, *11*(3), 1203–1216, doi:10.5194/acp-11-1203-2011.

Marple, V. A., K. L. Rubow, and S. M. Behm (1991), A Micro-orifice Uniform Deposit Impactor (MOUDI): Description, calibration, and use, *Aerosol Sci. Technol.*, *14*(4), 434–446, doi:10.1080/02786829108959504.

Mårtensson, E. M. (2003), Laboratory simulations and parameterization of the primary marine aerosol production, *J. Geophys. Res.*, *108*(D9), 4297, doi:10.1029/2002JD002263.

Modini, R. L., L. M. Russell, G. B. Deane, and M. D. Stokes (2013), Effect of soluble surfactant on bubble persistence and bubble-produced aerosol particles, *J. Geophys. Res. Atmos.*, *118*, 1388–1400, doi:10.1002/jgrd.50186.

Monahan, E. C., and I. G. O'Muircheartaigh (1986), Whitecaps and the passive remote sensing of the ocean surface, *Int. J. Remote Sens.*, *7*(5), 627–642, doi:10.1080/01431168608954716.

Norris, S. J., I. M. Brooks, M. K. Hill, B. J. Brooks, M. H. Smith, and D. A. J. Sproson (2012), Eddy covariance measurements of the sea spray aerosol flux over the open ocean, *J. Geophys. Res.*, *117*, D07210, doi:10.1029/2011JD016549.

O'Dowd, C. D., M. C. Facchini, F. Cavalli, D. Ceburnis, M. Mircea, S. Decesari, S. Fuzzi, Y. J. Yoon, and J.-P. Putaud (2004), Biogenically driven organic contribution to marine aerosol, *Nature*, *431*(7009), 676–680, doi:10.1038/nature02959.

O'Dowd, C. D., B. Langmann, S. Varghese, C. Scannell, D. Ceburnis, and M. C. Facchini (2008), A combined organic-inorganic sea-spray source function, *Geophys. Res. Lett.*, *35*, L01801, doi:10.1029/2007GL030331.

Quinn, P. K., T. S. Bates, K. S. Schulz, D. J. Coffman, A. A. Frossard, L. M. Russell, W. C. Keene, and D. J. Kieber (2014), Contribution of sea surface carbon pool to organic matter enrichment in sea spray aerosol, *Nat. Geosci.*, *7*, 228–232, doi:10.1038/ngeo2092.

Rinaldi, M., et al. (2013), Is chlorophyll-a the best surrogate for organic matter enrichment in submicron primary marine aerosol?, *J. Geophys. Res. Atmos.*, *118*, 4964–4973, doi:10.1002/jgrd.50417.

Salter, M. E., R. C. Upstill-Goddard, P. D. Nightingale, S. D. Archer, B. Blomquist, D. T. Ho, B. Huebert, P. Schlosser, and M. Yang (2011), Impact of an artificial surfactant release on air-sea gas fluxes during Deep Ocean Gas Exchange Experiment II, *J. Geophys. Res.*, *116*, C11016, doi:10.1029/2011JC007023.

Schkolnik, G., D. Chand, A. Hoffer, M. O. Andreae, C. Erlick, E. Swietlicki, and Y. Rudich (2007), Constraining the density and complex refractive index of elemental and organic carbon in biomass burning aerosol using optical and chemical measurements, *Atmos. Environ.*, *41*(5), 1107–1118, doi:10.1016/j.atmosenv.2006.09.035.

Skop, R. A., J. T. Viechnicki, and J. W. Brown (1994), A model for microbubble scavenging of surface-active lipid molecules from seawater, *J. Geophys. Res.*, *99*(C8), 16,395–16,402, doi:10.1029/94JC01199.

Stefan, R. L., and A. J. Szeri (1999), Surfactant scavenging and surface deposition by rising bubbles, *J. Colloid Interface Sci.*, *212*(1), 1–13, doi:10.1006/jcis.1998.6037.

Thorpe, S. A. (1982), On the clouds of bubbles formed by breaking wind-waves in deep water, and their role in air-sea gas transfer, *Philos. Trans. R. Soc. Lond. Ser. Math. Phys. Sci.*, *304*(1483), 155–210, doi:10.2307/36969.

Thorpe, S. A., and A. J. Hall (1983), The characteristics of breaking waves, bubble clouds, and near-surface currents observed using side-scan sonar, *Cont. Shelf Res.*, *1*(4), 353–384, doi:10.1016/0278-4343(83)90003-1.

Thorpe, S. A., A. R. Stubbs, A. J. Hall, and R. J. Turner (1982), Wave-produced bubbles observed by side-scan sonar, *Nature*, *296*(5858), 636–638, doi:10.1038/296636a0.

Tyree, C. A., V. M. Hellion, O. A. Alexandrova, and J. O. Allen (2007), Foam droplets generated from natural and artificial seawaters, *J. Geophys. Res.*, *112*, D12204, doi:10.1029/2006JD007729.

Vignati, E., G. de Leeuw, and R. Berkowicz (2001), Modeling coastal aerosol transport and effects of surf-produced aerosols on processes in the marine atmospheric boundary layer, *J. Geophys. Res.*, *106*(D17), 20,225–20,238.

Yoon, Y. J., et al. (2007), Seasonal characteristics of the physicochemical properties of North Atlantic marine atmospheric aerosols, *J. Geophys. Res.*, *112*, doi:10.1029/2005JD007044.

Zhou, X., A. J. Davis, D. J. Kieber, W. C. Keene, J. R. Maben, H. Maring, E. E. Dahl, M. A. Izaguirre, R. Sander, and L. Smoydzyn (2008), Photochemical production of hydroxyl radical and hydroperoxides in water extracts of nascent marine aerosols produced by bursting bubbles from Sargasso seawater, *Geophys. Res. Lett.*, *35*, L20803, doi:10.1029/2008GL035418.